

## Optically detected magnetic resonance study of relaxation/emission processes in the nanoparticle-polymer composite

G.Yu. Rudko<sup>1\*</sup>, I.P. Vorona<sup>1</sup>, V.M. Dzhagan<sup>1,2</sup>, A.E. Raevskaya<sup>3</sup>, O.L. Stroyuk<sup>3</sup>, V.I. Fediv<sup>4</sup>, A.O. Kovalchuk<sup>1</sup>, Jan E. Stehr<sup>5</sup>, WeiMin M. Chen<sup>5</sup>, I.A. Buyanova<sup>5</sup>

<sup>1</sup>V. Lashkaryov Institute of Semiconductor Physics of National Academy of Sciences of Ukraine, 45, prospect Nauky, 03680 Kyiv, Ukraine

<sup>2</sup>Taras Shevchenko National University of Kyiv, 01601 Kyiv, Ukraine

<sup>3</sup>L. Pysarzhevsky Institute of Physical Chemistry, National Academy of Sciences of Ukraine, 31, prospect Nauky, 03680 Kyiv, Ukraine

<sup>4</sup>Bukovinian State Medical University, Department of Biophysics and Medical Informatics, 42, Kobylyanska Str., 58000 Chernivtsi, Ukraine

<sup>5</sup>Department of Physics, Chemistry and Biology, Linkoping University, SE-581 83, Linkoping, Sweden

\*Corresponding author: g.yu.rudko@gmail.com

**Abstract.** Two nanocomposites containing CdS nanoparticles in polymeric matrices were studied using the photoluminescence (PL) and optically detected magnetic resonance (ODMR) methods. Due to equal sizes of NPs in the composites (~5 nm) but different matrices – the oxygen-containing polymer PVA (polyvinyl alcohol) and oxygen-free polymer PEI (polyethyleneimine) – differences of nanocomposites properties are predominantly caused by different interfacial conditions. ODMR spectra have revealed five types of centers related to the PL emission – four centers involved in radiative recombination and one center related to non-radiative recombination processes. The oxygen-related interfacial center in CdS/PVA (LK1-center) and sulfur vacancy center in CdS/PEI ( $V_s$ -center) were identified.

**Keywords:** CdS nanoparticles, polymer, composites, photoluminescence, optically detected magnetic resonance.

<https://doi.org/10.15407/spqeo22.03.310>

PACS 78.66.Sq, 76.70.Hb, 78.55.-m

Manuscript received 28.05.19; revised version received 16.06.19; accepted for publication 04.09.19; published online 16.09.19.

### 1. Introduction

Semiconductor nanoparticles (NPs) have been an object of extensive studies during at least four decades. The reasons for the acute research interest lie in the possibilities to vary the properties of NPs in a very wide range and, thus, to engineer the materials with pre-requisite characteristics suitable for diverse applications in numerous fields ranging from industry to medicine and from high tech to everyday life [1, 2]. The key sources for the tunability of the properties include the controllable variation of NPs sizes and adjusting surface conditions. The latter provides even wider variety of tuning possibilities, however, despite plenty of publications, the field is far from being well-understood.

The surface conditions of NPs are determined by the presence of dangling bonds, surface defects, local lattice distortions, and passivating ligands [3-6]. The latter are especially important for colloidal NPs because

surface termination with various types of capping agents is an inherent feature of the colloidal synthesis. By incorporating colloidal NPs into various matrices, the nanocomposites can be formed. In these systems, it is rather the NP/medium interface than the NP surface that contributes to the overall properties of a nanocomposite. All the above mentioned surface species together with the newly formed bonds between NPs and the molecules of the matrix can produce trapping states at the interface. These traps are critical for photoluminescent (PL) properties providing either radiative or non-radiative paths for recombination of excited electrons and holes.

PL spectra of NPs synthesized in aqueous media often feature broad band(s) that are highly red-shifted from the absorption edge [5, 7-10]. In many cases, the broadband PL emission of metal-chalcogenide NPs is interpreted in terms of a donor-acceptor pair (DAP) model [11]. This model assumes that the PL band width originates from a depth distribution of charge trap states,

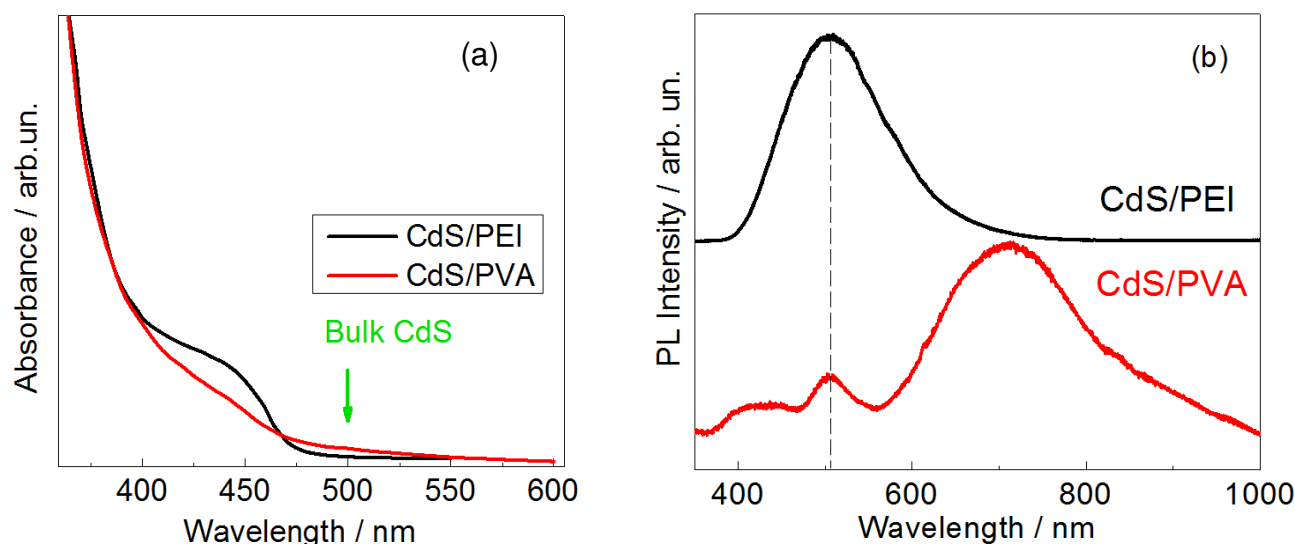


**Fig. 1.** (a) Absorption spectra of CdS NPs in PVA and PEI films; (b) PL spectra of CdS NPs in PEI (1) and PVA (2) matrices. The spectra are corrected to the spectral sensitivity of setup.

a size-dependence of the conduction and valence band positions in a polydisperse NP ensemble, as well as a distribution of distances between the trapped charge carriers within each sole NP. The DAP model meets a number of inconsistencies when being applied to ultra-small NPs (< 2 nm). Particularly, studies of single NPs revealed that their emission remains as broad as that of the ensemble [12, 13], undermining the argument of the PL width being determined by size distribution of NP, D-A distances and energy depths. Consequently, an alternative approach was proposed, based on self-trapped exciton model [14]. It assumes that PL originates from the vibrational relaxation of the interband excitation energy, which results in the broadband emission and dependence of the radiative lifetime on the PL energy [15], as was originally proposed for Si [16] and AgInS<sub>2</sub> NCs [17, 18] and later applied to doped II-VI NPs [14, 19].

What most of the works on NPs have in common is acknowledging the determinant role of the surface/interface on the optical properties of NPs, and a demand for knowing the exact nature of the recombination centers and charge traps in order to control these properties. However, establishing the nature of these electronic states is hardly possible by purely optical techniques. Despite ample spectroscopic optical studies, understanding of the direct relation of the interface structure and apparent optical properties of NP-based systems remains a challenge [12, 20, 21].

Here, we use the optically detected magnetic resonance (ODMR) method to identify paramagnetic centers that participate in the PL emission of NP-polymer nanocomposites. We studied two nanocomposites comprising CdS NPs embedded into two polymers – polyethylenimine (PEI) and polyvinyl alcohol (PVA). Both polymers are inexpensive, stable and readily available materials, which makes them attractive for

perspective large-scale nanocomposites production. Their transparency in the whole visible range and mechanical stability make them promising for optical applications [22-26]. Moreover, both polymers are bio-compatible and used for development of, e.g., drug-delivery and marker nanosystems, including the composites with semiconductor NPs [27, 28].

## 2. Materials and methods

### 2.1. Synthesis of nanocomposites

Both CdS/PVA and CdS/PEI nanocomposites were synthesized by the methods of colloidal chemistry at ambient conditions. In both cases, NPs were grown in an aqueous solution of the corresponding polymer via the reaction between Cd<sup>2+</sup> and HS<sup>-</sup>. All chemicals were analytical-grade (Sigma Aldrich) and were used without any additional purification.

Fabrication of CdS/PVA nanocomposites was made in 5 wt.% aqueous solution of PVA. The molecules of the basic polymer served as capping molecules that restricted sizes of the growing CdS NPs. Pending the growth process, the precursors (salts CdCl<sub>2</sub> and Na<sub>2</sub>S) were added step-wise to the growth solution thus sustaining concentrations of the precursors and pH values in ranges that ensured a gradual increase of NPs sizes and, simultaneously, eliminated formation of Cd(OH)<sub>2</sub>. Optimal ranges of these parameters were estimated by analyzing probabilities of possible chemical reactions in the solution as 10<sup>-4</sup>...10<sup>-2</sup> mol/L for the salts and pH = 3...5 [29]. Sulfur excess conditions were maintained during the growth.

The PEI-capped CdS NPs were synthesized using the method similar to that reported by us earlier [7, 8, 30], but with a new post-synthesis ripening step. As we reported [7, 8, 30], interaction between Cd<sup>2+</sup> and HS<sup>-</sup> ions in aqueous and ethanol solutions in the

presence of PEI results in very stable and monodisperse ultra-small CdS NPs with the average diameter 1.8 nm that are very similar to the well-reported magic-size (CdS)<sub>33</sub> clusters. These CdS-PEI NPs are characterized by a very sharp excitonic absorption maximum peaked at ~370 nm and a broadband PL emission centered around 500 nm. Here, we have found that addition of a combination of mercaptoacetic acid (MAA) and hydrazine results in the coarsening of CdS-PEI NPs and their gradual transformation into “ordinary” CdS NPs characterized by a continuous absorption band with an edge at ~470 nm (Fig. 1a) with no distinct absorption maxima. The most probable mechanism of this coarsening is the well-reported oriented attachment made possible, most probably, due to a competition of PEI with MAA and N<sub>2</sub>H<sub>4</sub> molecules for the undercoordinated Cd atoms on the surface of CdS NPs. We should note that detailed investigation of the mechanism of coarsening goes beyond the scope of the present paper and will be reported elsewhere.

In a typical synthesis of CdS-PEI NPs, 0.02 M CdCl<sub>2</sub> reacts with 0.01 M Na<sub>2</sub>S in aqueous 0.25 wt.% solution of PEI, as was described in detail in Refs. [7, 8, 30]. However, in the presence of 0.01 M MAA and 1.0 M hydrazine, the latter is introduced as hydrazine hydrate. The solution was kept in the dark at room temperature for 20 days to complete the coarsening of CdS NPs. After the coarsening, 2 wt.% gelatin was introduced into the solution acting as a film-forming agent. The gel obtained after gelatin introduction was poured onto a glass substrate cooled down to 5...7 °C and subjected to the dialysis against distilled water at this temperature for 30 min to remove the water-soluble residual salts. Then the gel was dried for 48 h at ambient conditions and natural air.

In synthesis of both CdS/PEI and CdS/PVA composites, the ratios of precursor concentrations and polymer content were adjusted to achieve almost equal size of CdS NPs grown in different matrices.

The films of CdS/PVA and CdS/PEI nanocomposites were obtained by depositing as-grown NP-containing polymeric solutions onto glass substrates with consequent drying at room temperature. The dried films were peeled off the substrates, and the free-standing films were used as samples for optical and ODMR measurements.

## 2.2. Experimental methods

PL emission of nanocomposites was excited using laser radiation (Coherent Verdi 2 W laser) with the wavelengths 266 or 390 nm and was detected by a 0.5-m Acton SpectraPro 2500i monochromator equipped with a CCD camera or Perkin-Elmer LS55 luminescence spectrometer. The PL spectra were measured at 5 K.

For ODMR measurements, a modified X band (microwave frequency ~9 GHz) EPR spectrometer was used. The PL signal was excited with a modulated 351 nm laser beam. ODMR signals were detected as changes in the PL intensity induced by modulating the microwave power. Typically, the microwave power was

200 mW. The lock-in technique was used for signal registration. The measurements were performed with a silicon detector at 5 K in a liquid helium flow cryostat. To analyze characteristics of ODMR signals, both spectrally-integrated measurements (by non-selective acquisition of the PL signal in the whole visible spectral range) and spectrally-selective measurements were made (the necessary spectral range was selected using suitable optical filters). The chosen spectral ranges are specified in the corresponding figures.

## 3. Results

Fig. 1 shows absorption (a) and PL (b) spectra of CdS/PEI and CdS/PVA nanocomposites. It is seen from Fig. 1a that the absorption edges of both nanocomposites are blue-shifted as compared to the band-to-band transitions in bulk CdS. This behavior results from the confinement of carriers in nanocrystals. The absorption spectrum of CdS/PEI exhibits a distinct absorption feature at about 450 nm corresponding to the lowest energy transitions between the levels of confined carriers. Using the energy position of this feature, the average size of NPs in CdS/PEI was calculated [30]. It was found to be approximately 5.0 nm. The corresponding feature is not clearly defined in the absorption spectrum of CdS/PVA, probably, due to larger distribution of NPs sizes. However, the sizes of NPs in these samples were previously determined using TEM in [31]. They are 5.4 nm. Thus, both types of nanocomposites under study contain NPs of approximately equal sizes.

As seen from Fig. 1b, both PL spectra demonstrate rather wide bands, which is typical for NPs synthesized in aqueous solutions [30, 32, 33]. It is seen that surface termination with different polymer molecules leads to drastically different emission properties of the composites, despite almost equal sizes of the embedded NPs. The CdS/PEI PL spectrum consists of a single broad and structureless band that covers the whole visible range (Fig. 1b). Correspondingly, the emission of CdS/PEI samples is seen by the naked eye as almost “white”. In the spectra of CdS/PVA samples, only a weak “green” band is observed, while a red-infrared band dominates the spectra. The resulting PL emission of the CdS/PVA samples is thus perceived by the naked eye as “yellowish-orange”. Thus, keeping in mind close sizes of NPs in both composites, the observed differences in the PL spectra evidence that the emission of NPs embedded into different matrices is strongly affected by matrix material and/or interfacial conditions. A common feature of the PL spectra of both composites is the large Stokes shift, which indicates that in both cases we are dealing with the recombination via deep levels.

According to our recent PL study of the CdS/PVA system, its emission spectrum contains four overlapping components: the blue band corresponding to residual emission from the polymeric matrix and three NP-related bands, one in the green region and two others in red and near IR ranges [34]. Even though no contribution of the PEI matrix to the PL spectrum of the CdS/PEI nanocomposite was established [7, 8, 30], the wide structureless

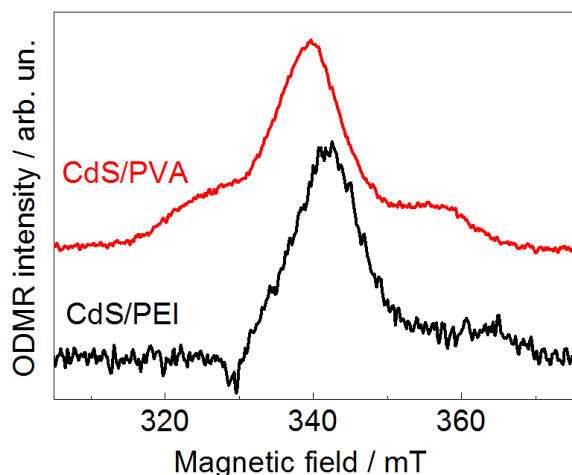


**Fig. 2.** ODMR spectra of CdS NPs in PEI and PVA matrices.

PL lineshape (Fig. 1b) prevents an unambiguous deconvolution of the monitored spectrum into several PL components solely based on optical measurements [7, 8, 30]. Therefore, the insight into the nature of PL emission is especially critical for this system.

Fig. 2 shows ODMR spectra of the CdS/PEI and CdS/PVA nanocomposites. In view of the fact that neither of polymeric matrices demonstrates ODMR signals, all the observed signals are only related to the paramagnetic centers located either inside NPs or at the NP/polymer interface. The spectra of both composites are complex, with three strongly overlapping components. In the case of CdS/PVA, these are the LK1, LK2, and LK3 signals already reported by us earlier [34]. All of them are positive. In the spectrum of CdS/PEI, two positive signals at higher fields resemble LK2 and LK3, while the signal at low magnetic field is specific for this system and is negative.

It should be noted that the amplitude of the ODMR signals in the CdS/PEI samples, 0.01%, is much smaller than that in CdS/PVA, ~1.0%. The latter value is rather high as compared to ODMR signals typically observed in bulk semiconductors and related nanostructures [35-39].

Notably, the ODMR signals in both types of nanocomposites are practically independent of the spectral range of optical detection. Fig. 3 shows the ODMR spectra of CdS/PVA (a) and CdS/PEI (b) measured within the spectral ranges labeled by the corresponding colors in the inserts. It is seen that the shapes of the ODMR spectra registered in different spectral ranges (Figs. 3a, 3b) as well as in the whole spectral range (Fig. 2) are almost the same.

#### 4. Discussion

Both studied nanocomposites contain NPs of almost equal sizes ( $\approx 5$  nm) made of the same CdS semiconductor. However, PL and ODMR spectra of these samples are different, which implies that the state of the interface and growth conditions play the crucial role in formation of nanocomposites properties.

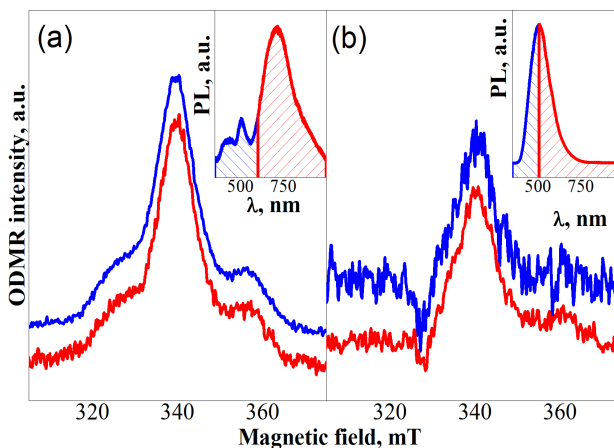


**Fig. 3.** ODMR spectra of CdS NPs in PVA (a) and PEI (b) matrices detected in the spectral ranges that are indicated with different colors on the corresponding PL spectra shown in the inserts.

The capping-dependent emission of CdS/PVA and CdS/PEI (Fig. 1) extends to energies well below the band edge, thus, it must be caused by defect-related recombination. In Ref. [34], it was suggested that at least two PL bands of CdS/PVA composite originate from the surface states. Therefore, the differences between CdS/PVA and CdS/PEI spectra should be analyzed with account of different matrices. Indeed, the structure of the nanoparticle/matrix interface obviously depends on the type of polymer. Polyvinyl alcohol, PVA, has the chemical formula  $(C_2H_4O)_n$ . Polyethyleneimine, PEI, has the chemical formula  $(C_2H_5N)_n$ . Thus, the nanocomposite CdS/PVA is an oxygen-containing substance, while in CdS/PEI nanocomposite oxygen can be present only as an uncontrolled impurity. Vice versa, there is plenty of nitrogen in CdS/PEI and, possibly, only traces of N in CdS/PVA. Both nitrogen and oxygen have unbound electron pairs, but N is a much stronger nucleophile and prone to form much stronger complexes with  $Cd^{2+}$ . Indications of coordination of PEI to Cd on NP surface were reported by us earlier [30]. Thus, NP surrounded by PEI should “feel” stronger negative charge pumped into NPs as compared to PVA. This may result in more efficient electron confinement in CdS-PEI NPs than in the same size NPs in PVA, thus reducing trapping of the confined electrons by the surface states.

Thus, two interfaces undoubtedly differ by the presence/absence of oxygen and nitrogen. Keeping in mind that both types of nanocomposites demonstrate similar “green” PL bands, though of dramatically different intensity (Fig. 1b), most probably the corresponding light-emitting centers are not related to either oxygen or nitrogen (note that “green” band in CdS/PVA was ascribed to surface in [34]). On the contrary, the emission in red and near-IR ranges, which dominates in CdS/PVA, may involve oxygen-containing interfacial centers.

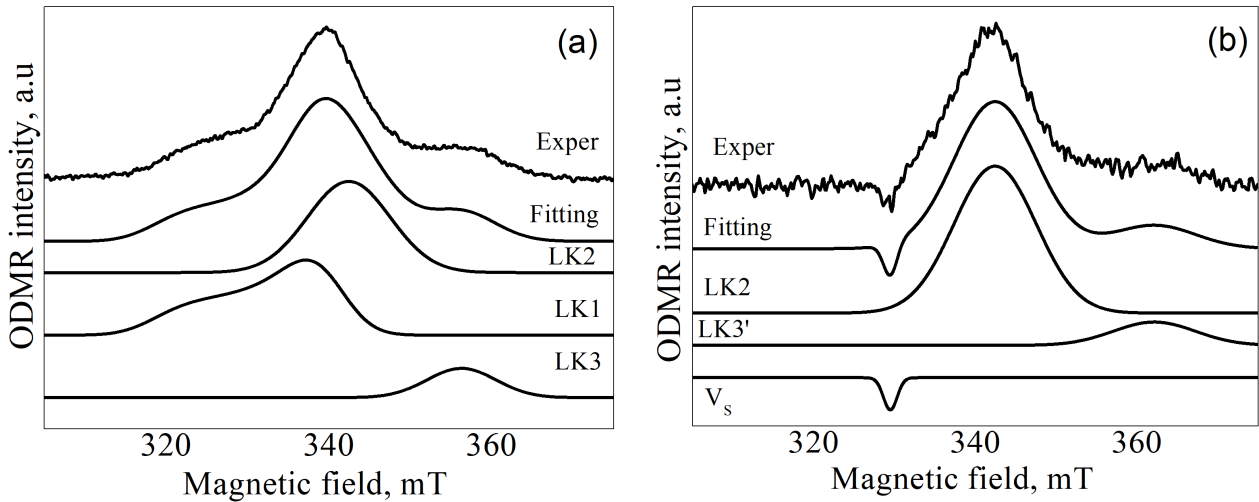


**Fig. 4.** Deconvolution of ODMR spectra of CdS NPs in PVA (a) and PEI (b) matrices. The fitting components are labeled as LK1, LK2, LK3 and LK3', the sum of all components is shown by the curve "Fitting", and the experimentally observed curve is labeled as "Exper".

Additional information on the role of matrix composition can be obtained from the ODMR studies. For the detailed analysis of ODMR spectra of CdS NPs in PEI and PVA matrices, we have made fitting of the corresponding spectra by using the spin Hamiltonian  $H = \mu_B \mathbf{B} \cdot \mathbf{g} \cdot \mathbf{S}$  with the effective electron spin  $\mathbf{S} = 1/2$ . Here,  $\mu_B$  is the Bohr magneton,  $\mathbf{B}$  is the external magnetic field,  $\mathbf{g}$  denotes the  $g$ -tensor. The fitting was performed for a powder system due to random orientations of NPs within the matrices. To model the ODMR spectra of CdS NPs in PVA, we used the LK1, LK2, and LK3 signals, as it was proposed in [34]. LK1 signal has the powder-like shape and corresponds to the anisotropic oxygen-related center, whereas LK2 and LK3 signals are caused by isotropic centers. LK1 and LK3 centers were interpreted as interface-related centers. The fitting parameters of the signals in Fig. 4 are as follows. LK1 signal was described using the  $g$ -values  $g_{\parallel} \sim 2.075$ ,  $g_{\perp} \sim 1.945$  and linewidth  $\Delta H = 4$  mT. LK2 and LK3 signals are isotropic with  $g \sim 1.93$ , and  $\sim 1.85$ , respectively. As can be seen from Fig. 4a, the results of fitting are in excellent agreement with the experimental data.

A similar fitting procedure was applied to the spectra of CdS/PEI. The results of the deconvolution are shown in Fig. 4b. To fit the ODMR spectra of CdS NPs in PEI, we omitted LK1, because no positive signal was observed in this range of magnetic fields. Instead, the negative signal labeled as  $V_s$  with the parameters  $g \sim 2.004$  and  $\Delta H = 1$  mT was used. A similar signal was previously observed in Ref. [40] and attributed to the sulfur vacancy in CdS. The appearance of this signal in the studied CdS/PEI nanocomposite is quite plausible, since the composite was synthesized under Cd-enriched

conditions, which may lead to formation of sulfur vacancies in NPs. To model the most intense signal in the spectrum of CdS/PEI, the same parameters as for LK2 center in Fig. 4a were used. However, the parameters of the third fitting component, which resembles the signal LK3 in the spectrum of CdS/PVA, were different from the LK3 parameters. Therefore, the third fitting component was described using the parameters  $g \sim 1.825$ ,  $\Delta H = 6$  mT and labeled as LK3'. It is seen that, similarly to the case of CdS/PVA, the fitted curve for CdS/PEI reasonably coincides with the experimental spectrum.

The comparison between the revealed ODMR centers in two types of structure shows that LK1 signal is present only in CdS/PVA nanocomposite. Previously, being based on anisotropy and values of spectroscopic parameters, we have suggested that this signal corresponds to the surface oxygen-related center similar to that discussed in Ref. [41]. Present observation additionally supports this suggestion, because LK1 signal is not seen in the spectrum of nanoparticles embedded into the polymer with no oxygen in its chemical formula. The parameters of LK1 differ from the parameters of the centers observed in [40], which is, probably, caused by different surroundings of these centers. This behavior resembles the strong dependence of oxygen centers parameters on local surrounding observed previously in [42-44].

Presence of identical LK2 signals in the ODMR spectra of both types of samples points to the occurrence of the same type of defects in these composites; they can occur either on the interface or inside NPs. The parameters of the high-field centers LK3 and LK3', despite being close, differ in two types of nanocomposites. Keeping in mind, that the  $g$ -factor of LK3

changed under the variation of surface conditions in [34], and is also affected by the nature of polymer capping in this work, we can tentatively suggest that LK2 and LK3' signals correspond to closely related centers or the same centers with slightly different surrounding. The  $g$ -factors of LK2, LK3 and LK3' are less than  $g$ -factor of the free electron, which points to the donor-like nature of these paramagnetic centers. However, at present we still have not enough data to propose possible models of the centers related to these signals.

We now discuss the role of the revealed defect centers in carrier recombination. The negative sign of the  $V_S$ -signal suggests that sulfur vacancies participate in recombination processes (either radiative or non-radiative) that compete with the visible emission. On the other hand, LK1, LK2 and LK3 signals in CdS/PVA, as well as LK2 and LK3' signals in CDS/PEI are positive. This means that all the corresponding paramagnetic centers are involved in the monitored radiative processes. However, the absence of the spectral dependence of these signals (Figs. 3a and 3b) implies that the corresponding paramagnetic centers are not the light-emitting ones. Thus, we suggest that these centers are involved at some intermediate stages preceding the radiative recombination, *e.g.*, they can introduce intermediate energy states within the band gap providing the path for a gradual loss of energy by carriers before being captured by light-emitting centers.

## 5. Conclusions

Two nanocomposites comprising CdS NPs in different polymeric matrices were studied using the photoluminescence and ODMR methods. The sizes of NPs in both composites were about 5 nm, the matrices were the oxygen-containing PVA (polyvinyl alcohol) and oxygen-free PEI (polyethyleneimine) polymers. Both nanocomposites exhibit wide-band defect-related luminescence, which is typical for NPs grown in water by using the colloidal methods. CdS/PEI has only one wide PL band that covers the whole visible range, whereas CdS/PVA has additional emissions in the near infrared range. Due to equal sizes of NPs in two composites, the differences in the properties were ascribed to different interfacial conditions.

ODMR study revealed the presence of three (two) paramagnetic centers in CdS/PVA (CdS/PEI) that participate in the processes leading to the monitored radiative recombination. Based on invariability of the ODMR spectra detected within different (green and red) spectral regions, the related paramagnetic centers were suggested to participate in energy relaxation processes preceding the emission rather than in light emission. One of these centers, LK1, was attributed to oxygen-related interfacial center in CdS/PVA. In addition, we have also showed that  $V_S$ -center is formed in CdS/PEI, and it is involved in carrier recombination processes competing with the visible emission in this material.

## Acknowledgement

This work is supported in parts by Volkswagen Foundation, Swedish Institute via Visby program and National Academy of Science of Ukraine (Project No. 26/18-H).

## References

1. Kovalenko M.V., Manna L., Cabot A. *et al.* Prospects of nanoscience with nanocrystals. *ACS Nano*. 2015. **9**. P. 1012–1057. <https://doi.org/10.1021/nn506223h>.
2. Pietryga J.M., Park Y.S., Lim J. *et al.* Spectroscopic and device aspects of nanocrystal quantum dots. *Chem. Rev.* 2016. **116**. P. 10513–10622. <https://doi.org/10.1021/acs.chemrev.6b00169>.
3. Harris R.D., Homan S.B., Kodaimati M. *et al.* Electronic processes within quantum dot-molecule complexes. *Chem. Rev.* 2016. **116**, Issue 21. P. 12865–12919. <https://doi.org/10.1021/acs.chemrev.6b00102>.
4. Krause M.M., Jethi L., Mack T.G., Kambhampati P. Ligand surface chemistry dictates light emission from nanocrystals. *J. Phys. Chem. Lett.* 2015. **6**. P. 4292–4296. <https://doi.org/10.1021/acs.jpcclett.5b02015>.
5. Baker D.R., Kamat P.V. Tuning the emission of CdSe quantum dots by controlled trap enhancement. *Langmuir*. 2010. **26**. P. 11272–11276. <https://doi.org/10.1021/la100580g>.
6. Sayevich V., Guhrenz C., Sin M. *et al.* Chloride and indium-chloride-complex inorganic ligands for efficient stabilization of nanocrystals in solution and doping of nanocrystal solids. *Adv. Funct. Mater.* 2016. **26**. P. 2163–2175. <https://doi.org/10.1002/adfm.201504767>.
7. Raevskaya A.E., Grodzyuk G.Y., Stroyuk A.L. *et al.* Preparation and spectral properties of high-efficiency luminescent polyethyleneimine-stabilized CdS quantum dots. *Theor. Exp. Chem.* 2010. **46**. P. 233–238. <https://doi.org/10.1007/s11237-010-9145-y>.
8. Dzhagan V.M., Valakh M.Y., Himcinschi C. *et al.* Raman and infrared phonon spectra of ultrasmall colloidal CdS nanoparticles. *J. Phys. Chem. C*. 2014. **118**. P. 19492–19497. <https://doi.org/10.1021/jp506307q>.
9. Smirnov M.S., Ovchinnikov O.V., Dedikova A.O. *et al.* Luminescence properties of hybrid associates of colloidal CdS quantum dots with J-aggregates of thiatrimethine cyanine dye. *J. Lumin.* 2016. **76**. P. 77–85. <https://doi.org/10.1016/j.jlumin.2016.03.015>.
10. Jing L., Kershaw S.V., Li Y. *et al.* Aqueous based semiconductor nanocrystals. *Chem. Rev.* 2016. **116**. P. 10623–10730. <https://doi.org/10.1021/acs.chemrev.6b00041>.
11. Chestnoy N., Harris T.D., Hull R., Brus L.E. Luminescence and photophysics of cadmium sulfide semiconductor clusters: the nature of the

- emitting electronic state. *J. Phys. Chem.* 1986. **90**. P. 3393–3399. <https://doi.org/10.1021/j100406a018>.
12. Dukes A.D., Samson P.C., Keene J.D. *et al.* Single-nanocrystal spectroscopy of white-light-emitting CdSe nanocrystals. *J. Phys. Chem. A*. 2011. **115**. P. 4076–4081. <https://doi.org/10.1021/jp1109509>.
  13. Whitham P.J., Marchioro A., Knowles K.E. *et al.* Single-particle photoluminescence spectra, blinking, and delayed luminescence of colloidal CuInS<sub>2</sub> nanocrystals. *J. Phys. Chem. C*. 2016. **120**. P. 17136–17142. <https://doi.org/10.1021/acs.jpcc.6b06425>.
  14. Stroyuk O. L., Raevskaya A. E., Gaponik N. *et al.* Origin of the broadband photoluminescence of pristine and Cu<sup>+</sup>/Ag<sup>+</sup>-doped ultra-small CdS and CdSe/CdS quantum dots. *J. Phys. Chem. C*. 2018. **122**. P. 10267–10277. <https://doi.org/10.1021/acs.jpcc.8b02337>.
  15. Mack T.G., Jethi L., Kambhampati P. Temperature dependence of emission line widths from semiconductor nanocrystals reveals vibronic contributions to line broadening processes. *J. Phys. Chem. C*. 2017. **21**. P. 28537–28545. <https://doi.org/10.1021/acs.jpcc.7b09903>.
  16. Kobitski A.Y., Zhuravlev K.S., Wagner H.P., Zahn D.R.T. Self-trapped exciton recombination in silicon nanocrystals. *Phys. Rev. B: Condens. Matter*. 2001. **63**. P. 115423. <https://doi.org/10.1103/PhysRevB.63.115423>.
  17. Hamanaka Y., Ogawa T., Tsuzuki M., Kuzuya T. Photoluminescence properties and its origin of AgInS<sub>2</sub> quantum dots with chalcopyrite structure. *J. Phys. Chem. C*. 2011. **115**. P. 1786–1792. <https://doi.org/10.1021/jp110409q>.
  18. Stroyuk O., Raevskaya A., Spranger F. *et al.* Origin and dynamics of highly-efficient broadband photoluminescence of aqueous glutathione-capped size-selected Ag-In-S quantum dots origin and dynamics of highly-efficient broadband photoluminescence of aqueous glutathione-capped size-selected Ag-In-S quantum dots. *J. Phys. Chem. C*. 2018. **122**, No 25. P. 13648–13658. <https://doi.org/10.1021/acs.jpcc.8b00106>.
  19. Knowles K.E., Nelson H.D., Kilburn T.B., Gamelin D.R. Singlet-triplet splittings in the luminescent excited states of colloidal Cu<sup>+</sup>:CdSe, Cu<sup>+</sup>:InP, and CuInS<sub>2</sub> nanocrystals: Charge-transfer configurations and self-trapped excitons. *J. Am. Chem. Soc.* 2015. **137**. P. 13138–13147. <https://doi.org/10.1021/jacs.5b08547>.
  20. Houtepen A.J., Hens Z., Owen J.S., Infante I. On the origin of surface traps in colloidal II-VI semiconductor nanocrystals. *Chem. Mater.* 2017. **29**. P. 752–761. <https://doi.org/10.1021/acs.chemmater.6b04648>.
  21. Mooney J., Krause M.M., Saari J.I., Kambhampati P. Challenge to the deep-trap model of the surface in semiconductor nanocrystals. *Phys. Rev. B*. 2013. **87**. P. 081201(R). <https://doi.org/10.1103/PhysRevB.87.081201>.
  22. Nakabayashi T., Wahadoszamen M., Ohta N. External electric field effects on state energy and photoexcitation dynamics of diphenylpolyenes. *J. Am. Chem. Soc.* 2005. **127**. P. 7041–7052. <https://doi.org/10.1021/ja0401444>.
  23. Borkovska L., Korsunska N., Stara T. *et al.* Enhancement of the photoluminescence in CdSe quantum dot-polyvinyl alcohol composite by light irradiation. *Appl. Surf. Sci.* 2013. **281**. P. 118–122. <https://doi.org/10.1016/j.apsusc.2012.12.146>.
  24. Mansur A.A.P., Ramanery F.P., Mansur H.S.. Water-soluble quantum dot/carboxylic-poly (vinyl alcohol) conjugates: insights into the roles of nanointerfaces and defects toward enhancing photoluminescence behavior. *Mater. Chem. Phys.* 2013. **141**. P. 223–233. <https://doi.org/10.1016/j.matchemphys.2013.05.004>.
  25. Mahmoud W.E., El-Mallah H.M. Synthesis and characterization of PVP-capped CdSe nanoparticles embedded in PVA matrix for photovoltaic application. *J. Phys. D: Appl. Phys.* 2009. **42**. P. 35502. <https://doi.org/10.1088/0022-3727/42/3/035502>.
  26. Pattabi M., Saraswathi A. B. Optical properties of CdS-PVA nanocomposites. *Compos. Interfaces*. 2010. **17**. P. 103–111. <https://doi.org/10.1088/0256-307X/30/5/057803>.
  27. Guan X., Fan H., Jia T. *et al.* A versatile synthetic approach to covalent binding of polymer brushes on CdSe/CdS quantum dots surface: multitype modification of nanocrystals. *Macromol. Chem. Phys.* 2016. **217**, No 5. P. 664–671. <https://doi.org/10.1002/macp.201500323>.
  28. Suo B., Su X., Wu J. *et al.* Poly (Vinyl Alcohol) thin film filled with CdSe-ZnS quantum dots: fabrication, characterization and optical properties. *Mater. Chem. Phys.* 2010. **119**. P. 237–242. <https://doi.org/10.1016/j.matchemphys.2009.08.054>.
  29. Kovalchuk A.O., Rudko G.Y., Fediv V.I., Gule E.G. Analysis of conditions for synthesis of CdS:Mn nanoparticles. *Semiconductor Physics, Quantum Electronics and Optoelectronics*. 2015. **18**. P. 74–78. <https://doi.org/10.15407/spqeo18.01.074>.
  30. Rayevska O.E., Grodzyuk G.Y., Dzhagan V.M. *et al.* Synthesis and characterization of white-emitting CdS quantum dots stabilized with polyethylenimine. *J. Phys. Chem. C* 2010. **114**. P. 22478–22486. <https://doi.org/10.1021/jp108561u>.
  31. Rudko G.Y., Kovalchuk A.O., Fediv V. I. *et al.* Role of the host polymer matrix in light emission processes in nano-CdS/poly vinyl alcohol composite. *Thin Solid Films*. 2013. **543**. P. 11–15. <https://doi.org/10.1016/j.tsf.2013.04.035>.
  32. Raevskaya A.E., Stroyuk O.L., Solonenko D.I. *et al.* Synthesis and luminescent properties of ultrasmall colloidal CdS nanoparticles stabilized by Cd(II) complexes with ammonia and mercaptoacetate. *J. Nanoparticle Res.* 2014. **16**. P. 2650. <https://doi.org/10.1007/s11051-014-2650-5>.

33. Raevskaya A.E., Stroyuk O.L., Panasiuk Y.V. *et al.* A new route to very stable water-soluble ultra-small core/shell CdSe/CdS quantum dots. *Nano-Structures & Nano-Objects*. 2018. **13**. P. 146–154. <https://doi.org/10.1016/j.nanos.2015.12.001>.
34. Rudko G.Yu., Vorona I.P., Fediv V.I. *et al.* Luminescent and optically detected magnetic resonance studies of CdS/PVA nanocomposite. *Nanoscale Res. Lett.* 2017. **12**. P. 130. <https://doi.org/10.1186/s11671-017-1892-4>.
35. Taylor P., Cavenett B.C. Optically Detected Magnetic Resonance (O. D. M. R.) investigations of recombination processes in semiconductors. *Adv. Phys.* 1981. **30**, No 4. P. 37–41. <https://doi.org/10.1080/00018738100101397>.
36. Wang X.J., Puttisong Y., Tu C.W. *et al.* Dominant recombination centers in Ga(In)NAs alloys: Ga interstitials. *Appl. Phys. Lett.* 2009. **95**. P. 95–98. <https://doi.org/10.1063/1.3275703>.
37. Stehr J.E., Dobrovolsky A., Sukrittanon S. *et al.* Optimizing GaNP coaxial nanowires for efficient light emission by controlling formation of surface and interfacial defects. *Nano Lett.* 2015. **15**. P. 242–247. <https://doi.org/10.1021/nl503454s>.
38. Dobrovolsky A., Stehr J.E., Chen S.L. *et al.* Mechanism for radiative recombination and defect properties of GaP/GaNP core/shell nanowires. *Appl. Phys. Lett.* 2012. **101**. P. 1–5. <https://doi.org/10.1063/1.4760273>.
39. Stehr J.E., Chen S.L., Filippov S. *et al.* Defect properties of ZnO nanowires revealed from an optically detected magnetic resonance study. *Nanotechnology*. 2013. **24**, No 1. P. 015701. <https://doi.org/10.1088/0957-4484/24/1/015701>.
40. Keeble D.J., Thomsen E.A., Stavrinadis A. *et al.* Paramagnetic point defects and charge carriers in PbS and CdS nanocrystal polymer composites. *J. Phys. Chem. C*. 2009. **113**. P. 17306–17312. <https://doi.org/10.1021/jp9044429>.
41. Sootha G.D., Padam G.K., Gupta S.K. Identification of oxygen radicals in CdS by ESR. *phys. status. solidi*. 1980. **58**. P. 615–622. <https://doi.org/10.1002/pssa.2210580235>.
42. Vorona I.P., Nosenko V.V., Baran N.P. *et al.* EPR study of radiation-induced defects in carbonate-containing hydroxyapatite annealed at high temperature. *Radiat. Meas.* 2016. **87**. P. 49–55. <https://doi.org/10.1016/j.radmeas.2016.02.020>.
43. Aseltine C.L., Kim Y.W. EPR studies of the thermal decay of the OH radicals in electron irradiated lithium sulfate at 77 K. *J. Phys. Chem. Solids*. 1968. **29**. P. 531–539. [https://doi.org/10.1016/0022-3697\(68\)90130-3](https://doi.org/10.1016/0022-3697(68)90130-3).
44. Känzig W., Cohen M.H. Paramagnetic resonance of oxygen in alkali halides. *Phys. Rev. Lett.* 1959. **3**. P. 509–510. <https://doi.org/10.1103/PhysRevLett.3.509>.

## Authors and CV



**Galyna Yu. Rudko**, Leading Researcher at the V. Lashkaryov Institute of Semiconductor Physics, NAS of Ukraine, Professor, Doctor of Sciences. The area of scientific interests includes optical and structural properties of semiconductors, related nanostructures and composite materials.



**Igor P. Vorona**, Leading researcher at the V. Lashkaryov Institute of Semiconductor Physics, NAS of Ukraine. The area of his scientific interests includes EPR, ODMR and ENDOR spectroscopy, defects in solids.



**Volodymyr M. Dzhagan**, Senior Researcher at the V. Lashkaryov Institute of Semiconductor Physics, NAS of Ukraine, Doctor of Sciences. The area of scientific interests includes optical and vibrational properties of semiconductors, related nanostructures and composite materials.



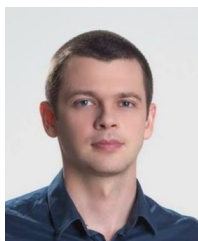
**Alexandra E. Raevskaya**, Senior Researcher at the L.V. Pysarzhevsky Institute of Physical Chemistry, NAS of Ukraine, PhD. The area of scientific interests includes synthesis and photochemistry of colloidal semiconductor nanocrystals and related nanostructures and composite materials.



**Oleksandr L. Stroyuk**, Senior Researcher at the L.V. Pysarzhevsky Institute of Physical Chemistry, NAS of Ukraine, Doctor of Sciences. The area of scientific interests includes synthesis and photochemistry of colloidal semiconductor nanocrystals and related nanostructures and composite materials.



**Volodymyr I. Fediv**, Professor, Doctor of Physical and Mathematical Sciences, Head of the Department of Biological Physics and Medical Informatics of Bukovinian State Medical University (Chernivtsi, Ukraine) from 2015. He is the author of more than 40 scientific articles, 100 scientific and teaching auctions, 2 patents and 17 teaching aids.



**Andrii O. Kovalchuk**, at 2016 defended PhD thesis on the topic “Optical and electrical properties of polymer composite with CdS nanoparticles”. Junior researcher at the V. Lashkaryov Institute of Semiconductor Physics, NAS of Ukraine. He have done researches at Division of Functional Electronic Materials,

The Department of Physics, Chemistry and Biology, Linköping University, Sweden as a member of Ukrainian-Swedish Visby Research Program at 2011-2013.



**Jan E. Stehr**, in 2006–2011 worked at Justus-Liebig-Universität Gießen, Physical Institute, Germany, Gießen. Since 2012 till now Senior Lecturer, Researcher at the Department of Physics, Chemistry and Biology, Institute of Functional Materials, Linköping University, Linköping, Sweden. Scientific interest: surface physics and chemistry.



**WeiMin M. Chen**, Director of the Swedish Interdisciplinary Magnetic Resonance Center (SIMARC) and Head of the Division of Functional Electronic Materials, Department of Physics, Chemistry and Biology, Linköping, Sweden. In 1991-1993 was a post-doctoral researcher at Department of Materials Science and Engineering University of California, Berkeley, USA.



**Irina A. Buyanova**, Professor in the research unit of Functional electronic materials, Department of Physics, Chemistry and Biology, Linköping University, Linköping, Sweden. Area of scientific interest: physics and applications of advanced electronic and photonic materials based on wide-bandgap and highly mismatched semiconductors and related nanostructures,

novel spintronic semiconductor materials, electronic and material-related properties of two-dimensional semiconductors.